Phys. Lett. B 850 (2024) 138539

Contents lists available at ScienceDirect

Physics Letters B

journal homepage: www.elsevier.com/locate/physletb

Letter

NLO EW corrections to polarised W^+W^- production and decay at the LHC

Ansgar Denner [a], Christoph Haitz [a], Giovanni Pelliccioli [b,*]

[a] University of Würzburg, Institut für Theoretische Physik und Astrophysik, Emil-Hilb-Weg 22, 97074 Würzburg, Germany
[b] Max-Planck-Institut für Physik, Bolzmannstrasse 8, 85748 Garching, Germany

ARTICLE INFO

Editor: G.F. Giudice

Keywords:
Polarisation
NLO
Electroweak
LHC

ABSTRACT

In this letter we present results for next-to-leading-order electroweak corrections to doubly polarised W^+W^- production at the LHC in the fully leptonic decay channel. We model the production and the decay of two polarised W bosons in the double-pole approximation, including factorisable real and virtual electroweak corrections, and separating polarisation states at amplitude level. We obtain integrated and differential predictions for polarised signals in a realistic fiducial setup.

1. Introduction

Separating polarisation modes of W and Z bosons and extracting the longitudinal one represents an important step towards the complete understanding of the interplay between the electroweak (EW) and Higgs sector of the Standard Model (SM). Any deviation from the SM prediction for the production rate of longitudinally polarised EW bosons in LHC processes would signal the presence of new-physics effects pointing to a modified structure of the EW-symmetry-breaking mechanism compared to the SM one.

Though challenging, the extraction of polarisation fractions of EW bosons from LHC data has already been achieved with the Run-2 dataset [1–5], and more results are expected from the Run-3 and High-Luminosity stages. The current analysis strategies for diboson inclusive production [1,3–5] and scattering [2] are based on data fits performed with independent templates for the various polarised signals. This is made possible by the definition of polarised cross sections, *i.e.* cross sections for fixed polarisation of intermediate EW bosons, and their numerical simulation with Monte Carlo codes. The recent theoretical progress has led to accurate and precise SM predictions for inclusive polarised diboson production in the fully leptonic decay channel, achieving next-to-leading order (NLO) QCD accuracy for all diboson channels [6–9], next-to-next-to-leading order (NNLO) QCD accuracy for W^+W^- [10], and NLO QCD+EW accuracy for ZZ [11] and WZ [12–14] production.

The inclusive production of a pair of leptonically decaying W bosons at the LHC is the most challenging diboson channel from the experimental point of view, owing to the large top-quark backgrounds and the cumbersome reconstruction of the final state with two undetected neutrinos. The SM differential cross section for off-shell W^+W^- production is known up to NNLO QCD [15–17] and NLO EW [17–19] perturbative accuracy, also matched to parton shower [20–22]. In the case of intermediate polarised bosons, the NLO [6] and NNLO [10] QCD corrections are known, and the matching of NLO QCD ones to a parton shower has been achieved recently [23].

In this work we extend the SM modelling of doubly polarised W^+W^- production to the inclusion of NLO EW corrections in the decay channel with two charged leptons of different flavours. We stress that these corrections represent the last missing building blocks for the SM modelling at complete NLO EW+QCD accuracy of polarised boson-pair production in all possible leptonic decay channels.

In our approach, polarised cross sections are defined after selecting doubly resonant contributions (containing two resonant W bosons) and projecting their momenta on shell (to guarantee gauge independence). The difference between the doubly resonant contributions and the full calculation (containing less than two resonant W bosons) is considered as an irreducible background that should be fitted simultaneously with the polarised cross sections. Similarly, the (doubly resonant) interference contributions should be considered as a separate contribution to be included in the fits if necessary. For more details of our approach we refer to Refs. [6,11].

This letter is organised as follows. In Section 2 we describe the main features of the NLO EW calculation. The setup for numerical simulations is summarised in Section 3, and the corresponding results are discussed in Section 4. In Section 5 we draw our conclusions.

* Corresponding author.
E-mail addresses: ansgar.denner@uni-wuerzburg.de (A. Denner), christoph.haitz@uni-wuerzburg.de (C. Haitz), gpellicc@mpp.mpg.de (G. Pelliccioli).

https://doi.org/10.1016/j.physletb.2024.138539
Received 1 December 2023; Received in revised form 11 January 2024; Accepted 17 February 2024
Available online 23 February 2024

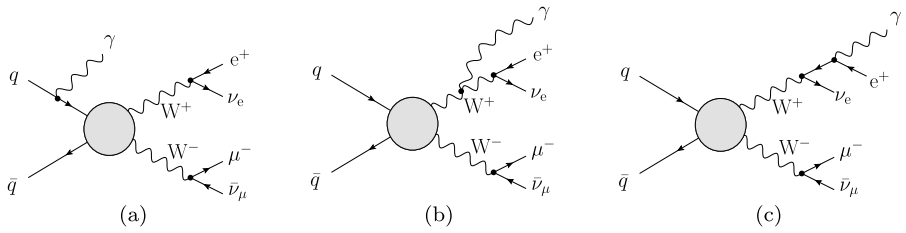

Fig. 1. Sample photon-radiation diagrams contributing to W^+W^- production and decay at NLO EW.

2. Details of the calculation

We consider the production and decay of two W bosons at NLO EW accuracy, specifically

$$\mathrm{pp} \to \mathrm{e}^+\nu_\mathrm{e}\mu^-\bar{\nu}_\mu + X\,. \tag{1}$$

In the five-flavour scheme, the channels

$$q\bar{q},\, \mathrm{b\bar{b}},\, \gamma\gamma \to \mathrm{e}^+\nu_\mathrm{e}\mu^-\bar{\nu}_\mu\,, \tag{2}$$

($q = \mathrm{u}, \mathrm{d}, \mathrm{s}, \mathrm{c}$) are present at LO, and at NLO EW accuracy the contributing real channels read

$$\begin{aligned} &q\bar{q},\, \mathrm{b\bar{b}}\,, \gamma\gamma \to \mathrm{e}^+\nu_\mathrm{e}\mu^-\bar{\nu}_\mu\gamma\,,\\ &\qquad \gamma\overset{(-)}{q} \to \mathrm{e}^+\nu_\mathrm{e}\mu^-\bar{\nu}_\mu\overset{(-)}{q}\,,\\ &\qquad \gamma\overset{(-)}{\mathrm{b}} \to \mathrm{e}^+\nu_\mathrm{e}\mu^-\bar{\nu}_\mu\overset{(-)}{\mathrm{b}}\,. \end{aligned} \tag{3}$$

In the full off-shell calculation, the complete set of real and virtual diagrams is taken into account.

For unpolarised and doubly polarised signals, we carry out the calculation in the double-pole approximation (DPA) [24–27], including only factorisable real and virtual EW corrections. The DPA approach has already been used for the simulation of polarised intermediate EW bosons in diboson LHC processes at NLO QCD [6–8], NNLO QCD [10], and NLO EW [11–13] accuracy.

The $\gamma\mathrm{b}\,(\gamma\bar{\mathrm{b}})$ channels embed (anti)top quarks in the s channel, and should therefore be regarded as an irreducible background to the W^+W^- EW production. Therefore, while included as a contribution to the full off-shell calculation as a reference, these contributions are excluded from the DPA calculations (polarised and unpolarised), *i.e.* we assume a perfect b-jet veto. Experimentally, this background could as well be subtracted based on a template fit.

In the DPA, the Born-like contributions (Born, virtual, and subtraction counterterms) are characterised by two W bosons undergoing two-body decays,

$$q\bar{q},\, \mathrm{b\bar{b}},\, \gamma\gamma \to \mathrm{W}^+(\mathrm{e}^+\nu_\mathrm{e})\,\mathrm{W}^-(\mu^-\bar{\nu}_\mu), \tag{4}$$

where the notation $\mathrm{W}^+(\mathrm{e}^+\nu_\mathrm{e})$ denotes a W^+ boson decaying into $\mathrm{e}^+\nu_\mathrm{e}$. The same holds for real corrections with an additional particle, a photon or a quark, radiated off the production part of the process,

$$\begin{aligned} &q\bar{q},\, \mathrm{b\bar{b}},\, \gamma\gamma \to \mathrm{W}^+(\mathrm{e}^+\nu_\mathrm{e})\,\mathrm{W}^-(\mu^-\bar{\nu}_\mu)\,\gamma\,,\\ &\qquad \gamma\overset{(-)}{q} \to \mathrm{W}^+(\mathrm{e}^+\nu_\mathrm{e})\,\mathrm{W}^-(\mu^-\bar{\nu}_\mu)\overset{(-)}{q}\,,\\ &\qquad \gamma\overset{(-)}{b} \to \mathrm{W}^+(\mathrm{e}^+\nu_\mathrm{e})\,\mathrm{W}^-(\mu^-\bar{\nu}_\mu)\overset{(-)}{b}\,. \end{aligned} \tag{5}$$

Following Ref. [11], these contributions are treated with the DPA(2,2) mapping, *i.e.* a projection of the momenta for the processes $q\bar{q},\, \mathrm{b\bar{b}},\, \gamma\gamma \to \mathrm{e}^+\nu_\mathrm{e}\mu^-\bar{\nu}_\mu$ to momenta for the processes $q\bar{q},\mathrm{b\bar{b}},\gamma\gamma \to \mathrm{W}^+\mathrm{W}^- \to \mathrm{e}^+\nu_\mathrm{e}\mu^-\bar{\nu}_\mu$ with on-shell W bosons.[1] A photon can be also emitted off the decay products of a W boson, leading to a resonant structure with one two-body and one three-body decay,

$$\begin{aligned} &q\bar{q},\, \mathrm{b\bar{b}},\, \gamma\gamma \to \mathrm{W}^+(\mathrm{e}^+\nu_\mathrm{e}\gamma)\,\mathrm{W}^-(\mu^-\bar{\nu}_\mu),\\ &q\bar{q},\, \mathrm{b\bar{b}},\, \gamma\gamma \to \mathrm{W}^+(\mathrm{e}^+\nu_\mathrm{e})\,\mathrm{W}^-(\mu^-\bar{\nu}_\mu\gamma)\,. \end{aligned} \tag{6}$$

According to the notation of Ref. [11], these contributions are treated with the DPA(3,2) and DPA(2,3) mappings, respectively, *i.e.* projections of the momenta for the processes $q\bar{q},\, \mathrm{b\bar{b}},\, \gamma\gamma \to \mathrm{e}^+\nu_\mathrm{e}\mu^-\bar{\nu}_\mu\gamma$ (with an extra photon) to momenta for the processes $q\bar{q},\, \mathrm{b\bar{b}},\, \gamma\gamma \to \mathrm{W}^+\mathrm{W}^- \to \mathrm{e}^+\nu_\mathrm{e}\mu^-\bar{\nu}_\mu\gamma$ with on-shell W bosons, where the first/second W boson decays into two leptons and a photon and the second/first one into two leptons.

The infrared singularities of QED origin are subtracted in the dipole formalism [28–32]. Compared to the full off-shell calculation, where emitters and spectators of the dipoles are charged massless particles in the initial or final state, the DPA calculations require a tailored dipole selection, owing to the separate treatment of the production and decay of the resonances. This procedure is especially delicate for the soft-photon singularities that arise from the emission of photons off W bosons whose momenta have been projected on mass shell through a DPA mapping. In order to further detail the DPA approach used for our calculation, we consider the real partonic process $q\bar{q} \to \mathrm{e}^+\nu_\mathrm{e}\mu^-\bar{\nu}_\mu\gamma$. The contributing diagrams in the DPA can feature a photon that is radiated off the production part of the amplitude, from a W-boson propagator, or from the decay part of the amplitude. Since diagrams like the one depicted in Fig. 1(a) contain a photon radiated off initial-state (IS) quarks or antiquarks, they only contribute to the production process of two W bosons. These diagrams give rise to soft and collinear singularities, which in the dipole formalism are absorbed by IS–IS and IS–FS dipoles, where either another quark or antiquark (IS–IS) or one of the two W bosons (IS–FS) plays the role of the spectator. The second class of diagrams [Fig. 1(b)] is characterised by a photon emitted off an s-channel W boson and embeds singularities associated both with the production side and with the decay side of the amplitude, treated separately by means of a partial fractioning [33,34]. This gives rise to FS–IS (W boson as emitter, incoming parton as spectator) and FS–FS dipoles (one W boson is the emitter, the other W is the spectator) to absorb production-level singularities, and a decay dipole for the decay-level singularities. The last class of diagrams [Fig. 1(c)] contains a photon emitted from a charged lepton, whose singularity is absorbed by a decay dipole. Following the strategy proposed in Ref. [12], for the production-level dipoles with a W boson as emitter and/or spectator (FS–FS, FS–IS, IS–FS) the massive-fermion dipoles [30] are employed. This is possible, since owing to the finite mass of the W boson no spin-dependent collinear singularities are present in the photon radiation from the W bosons. Compared to WZ inclusive production [12,13], the novel structures needed for this calculation are the FS–FS dipoles with equal masses (M_W) that we implemented as a simplified version of the corresponding structures in Ref. [30]. For the W-boson decay, we have devised a single dipole that reproduces the exact structure of the real $\mathrm{W} \to \ell\nu_\ell\gamma$ matrix element and that could be analytically integrated in $4 - 2\epsilon$ dimensions. This dipole absorbs the singularities related to photon emission both from the W boson and from the decay lepton.

[1] The numbers in DPA(2,2) refer to the numbers of decay particles/momenta of the two vector bosons.

The sum of integrated counterterms for the production part (taken from Ref. [30]) and decay (integrated version of our W-decay kernel) has been proven to reproduce the explicit infrared poles of the factorisable virtual corrections. The contribution of non-factorisable soft-photon corrections of virtual origin is expected to be small and to cancel to a large extent against the corresponding real corrections [35]. Therefore we exclude them from this work and leave them for future investigation.

The calculation strategy described above for real and virtual contributions as well as for the local and integrated counterterms has been applied to the unpolarised process and to the doubly polarised ones. This allows the selection of individual polarisation contributions in the two W-propagator numerators, following the general strategy proposed in Ref. [6] and already applied at NLO EW to ZZ [11] and WZ inclusive production [12–14].

At variance with the choice made in other fixed-order results in the literature [6,10], the polarisation states for the two W bosons are defined in the diboson centre-of-mass (CM) frame, which is regarded as the most natural Lorentz frame for the definition of vector-boson polarisations in diboson processes [7,11–14].

The calculation has been performed independently with the BBMC and MoCaNLO Monte Carlo codes, both of which have already been used for the simulation of intermediate polarised bosons at NLO accuracy [6–8,11]. The two codes have been interfaced with the latest release (1.4.4) of the Recola library [36,37] that enables the calculation of tree-level and one-loop amplitudes with fixed polarisation states for intermediate resonances. The reduction and integration of one-loop amplitudes in Recola is achieved through the Collier library [38]. A number of checks have been performed to verify the correctness of fixed-helicity amplitudes by means of variations of the UV regulator in Recola, comparisons against analytic results, and independent numerical results obtained with MadLoop [39]. All integrated and differential results provided in this letter are computed with MoCaNLO and have been checked against BBMC, finding agreement within numerical-integration uncertainties.

3. Setup

The simulations are performed at a centre-of-mass energy of $\sqrt{s} = 13.6\,\text{TeV}$ for proton–proton collisions at the LHC. The on-shell masses and widths of the EW bosons have been set to the values [40],

$$\begin{aligned} M_\text{Z}^\text{OS} &= 91.1876\,\text{GeV}, & \Gamma_\text{Z}^\text{OS} &= 2.4952\,\text{GeV}, \\ M_\text{W}^\text{OS} &= 80.377\,\text{GeV}, & \Gamma_\text{W}^\text{OS} &= 2.085\,\text{GeV}, \end{aligned} \tag{7}$$

and then converted to their corresponding pole values [41]. The top-quark and Higgs-boson mass and width are fixed as [40],

$$\begin{aligned} m_\text{t} &= 172.69\,\text{GeV}, & \Gamma_\text{t} &= 1.42\,\text{GeV}, \\ M_\text{H} &= 125.25\,\text{GeV}, & \Gamma_\text{H} &= 0.0041\,\text{GeV}. \end{aligned} \tag{8}$$

The G_μ scheme [27,42] is employed to determine the EW coupling. In formulas,

$$\alpha = \frac{\sqrt{2}}{\pi} G_\mu \left| \hat{M}_\text{W}^2 \left(1 - \frac{\hat{M}_\text{W}^2}{\hat{M}_\text{Z}^2} \right) \right| \tag{9}$$

for the full off-shell calculation in the complex-mass scheme [34,43,44], where $\hat{M}_V^2 = M_V^2 - \text{i} M_V \Gamma_V$ ($V = \text{W}, \text{Z}$), while

$$\alpha = \frac{\sqrt{2}}{\pi} G_\mu M_\text{W}^2 \left(1 - \frac{M_\text{W}^2}{M_\text{Z}^2} \right) \tag{10}$$

for the DPA calculations. The Fermi constant is set to

$$G_\mu = 1.16638 \times 10^{-5}\,\text{GeV}^{-2}, \tag{11}$$

and M_Z, M_W and $\Gamma_\text{W}, \Gamma_\text{Z}$ represent the pole values for the weak-boson masses and widths, respectively.

We perform the calculation in the five-flavour scheme, including partonic channels induced by bottom (anti)quarks and photons. The PDF set `NNPDF31_nnlo_as_0118_luxqed` [45,46] has been utilised through the LHAPDF interface [47]. The renormalisation and factorisation scales are both set to the W pole mass,

$$\mu_\text{R} = \mu_\text{F} = M_\text{W}. \tag{12}$$

The selections used throughout this paper mimic those of a recent CMS measurement [48] (dubbed *sequential-cut selections* therein). The charged leptons are dressed with photon radiation according to anti-k_T clustering algorithm [49] with resolution radius $R = 0.1$. The final state must satisfy

$$\begin{aligned} & p_{\text{T},\ell_1} > 25\,\text{GeV}, \quad p_{\text{T},\ell_2} > 20\,\text{GeV}, \\ & |\eta_{\text{e}^+}| < 2.5, \quad |\eta_{\mu^-}| < 2.4, \\ & p_{\text{T},\text{e}^+\mu^-} > 30\,\text{GeV}, \quad M_{\text{e}^+\mu^-} > 20\,\text{GeV}, \\ & p_{\text{T,miss}} > 20\,\text{GeV}, \end{aligned} \tag{13}$$

where $\ell_{1,2}$ are the leading and subleading charged leptons ordered according to their transverse momenta.

Throughout the whole paper we use the labels L and T for longitudinal and transverse polarisation, respectively. When discussing doubly polarised states (LL, LT, TL, and TT), the first index refers to the W^+ boson, the second one to the W^- boson.

4. Results

In this section we present integrated and differential results at NLO EW order in the fiducial setup defined in Eq. (13). Since we are interested in assessing the impact of EW radiative corrections, we do not show QCD-scale uncertainties which in our calculation would only come from factorisation-scale variations. A realistic estimate of QCD-scale uncertainties would require at least the inclusion of NLO QCD corrections, which has been recently carried out [23] in a similar setup as the one considered in this work, finding 3–5% uncertainties with mild differences among various polarised states.

In Table 1 we show fiducial cross sections at LO and NLO EW accuracy for the full, unpolarised, and doubly polarised W^+W^- signals. The results are presented both with and without the $\text{b}\bar{\text{b}}$ channel. In the case of the full calculation, we also assess the impact of the $\gamma\text{b}(\gamma\bar{\text{b}})$ channels, which differ from the corresponding ones with light quarks by the presence of (anti)top-quark propagators in the s channel. Excluding all bottom-induced contributions, the TT state gives by far the largest fraction to the unpolarised signal while the purely longitudinal state amounts to 7.7% of the total at NLO EW. The differences between the TL and LT polarisations originate from the differences in PDFs between quarks and antiquarks. The off-shell effects, evaluated from the difference between the full and unpolarised cross sections, are at the 3.5% level, in agreement with the intrinsic uncertainty of the DPA. The striking effect is the size of interferences among polarisation states (−8%), evaluated from the difference between the unpolarised and sum of polarised cross sections. This effect, already observed in previous W^+W^- calculations [6,10,23], comes from the application of transverse-momentum cuts on the two charged leptons, which prevents the interference between longitudinal and transverse modes of both bosons from vanishing. It is especially large for W bosons, whose left-chiral coupling to fermions induces a dramatic change in the decay-angle shapes in the most populated region (anticollinear and collinear, respectively for the W^+ and W^- bosons), when applying fiducial cuts (compared to a fully inclusive setup). The effect of the cuts is also visible in Fig. 2. The NLO EW corrections are negative and different for the various polarised and unpolarised states. In particular, their size is maximal for the TT state (−2.4%), smaller for the LL one (−1.3%). Almost

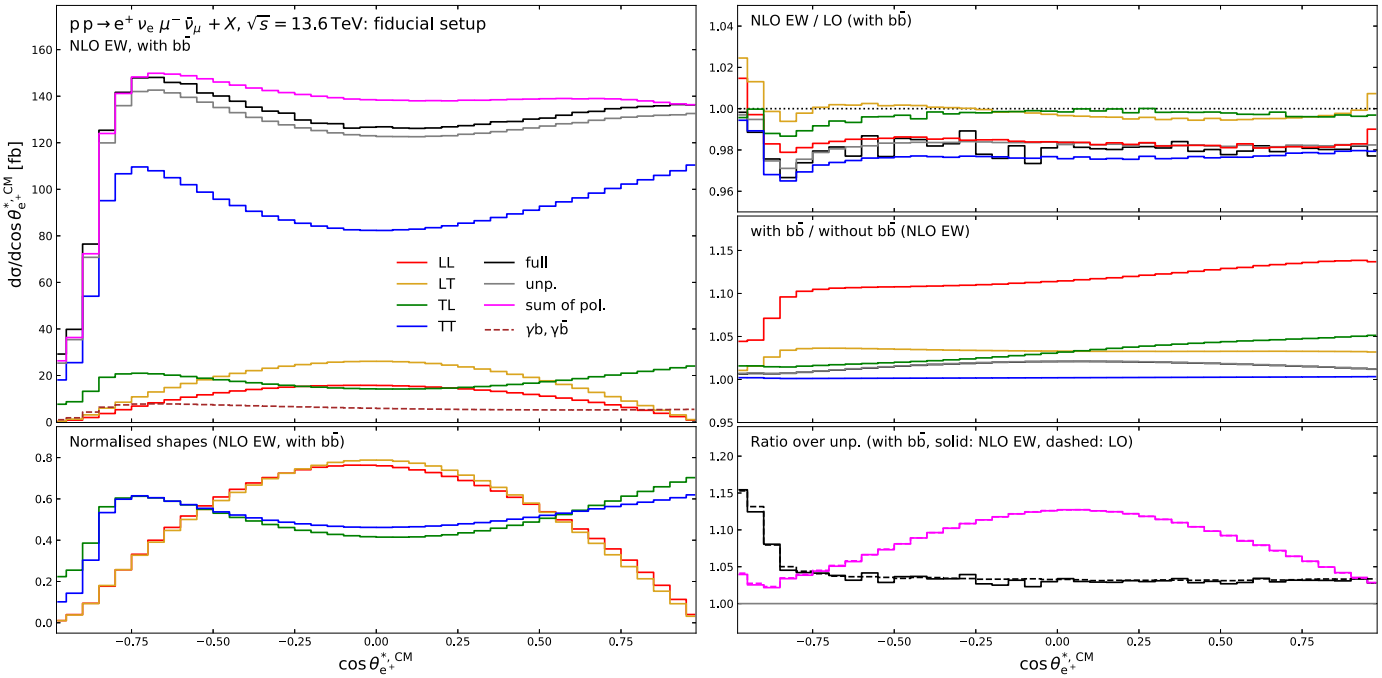

Fig. 2. Distributions in the polar decay angle of the positron in the W^+ rest frame for W^+W^- production and decay at the LHC with NLO EW accuracy. The setup detailed in Section 3 is understood. Polarisations are defined in the diboson CM reference frame. Colour key: full off-shell (black), unpolarised (gray), LL (red), LT (yellow), TL (green), TT (blue), sum of doubly polarised (magenta), $\gamma b\,(\gamma\bar{b})$ contributions (brown, dashed). Left panel: absolute differential distributions (top) and normalised shapes (bottom) at NLO EW, including $b\bar{b}$ contributions. Right panel: ratios of NLO EW results over the LO ones, including $b\bar{b}$ contributions (top), ratios of NLO EW cross sections with and without $b\bar{b}$ contributions included (middle), ratios of cross sections over the unpolarised ones at LO and NLO EW (bottom).

Table 1
Fiducial cross sections (in fb) at LO and NLO EW for full, unpolarised, and doubly polarised W^+W^- production at the LHC in the fully leptonic decay channel. Absolute numbers in parentheses are numerical integration uncertainties. The value $\delta_{\rm EW}$ (in percentage) is computed as the EW correction relative to the LO result. The values $f_{\rm NLOEW}$ are fractions of NLO EW cross sections over the NLO EW unpolarised result. The γb, $\gamma\bar{b}$ contributions are only included in the full calculation (last row). The interference (int.) is evaluated as the difference between the unpolarised and the sum of polarised results.

state	$\sigma_{\rm LO}$ [fb]	$\sigma_{\rm NLOEW}$ [fb]	$\delta_{\rm EW}$[%]	$f_{\rm NLOEW}$[%]
$b\bar{b}$, γb, $\gamma\bar{b}$ excluded				
full	254.79(2)	249.88(9)	−1.93	103.5
unp.	245.79(2)	241.48(2)	−1.75	100
LL	18.752(2)	18.510(2)	−1.30	7.7
LT	32.084(3)	32.043(3)	−0.13	13.3
TL	33.244(5)	33.155(5)	−0.27	13.7
TT	182.17(2)	177.83(2)	−2.38	73.6
int.	−20.46(3)	−20.1(1)	−1.96	−8.3
$b\bar{b}$ included, γb, $\gamma\bar{b}$ excluded				
full	259.02(2)	253.95(9)	−1.96	103.4
unp.	249.97(2)	245.49(2)	−1.79	100.0
LL	21.007(2)	20.663(2)	−1.64	8.4
LT	33.190(3)	33.115(3)	−0.23	13.5
TL	34.352(5)	34.230(5)	−0.35	13.9
TT	182.56(2)	178.21(3)	−2.38	72.6
int.	−21.14(5)	−20.6(2)	−2.45	−8.4
$b\bar{b}$, γb, $\gamma\bar{b}$ included				
full	259.02(2)	265.59(9)	+2.54	-

negligible EW corrections are found for the mixed polarisation states (LT, TL).

The inclusion of $b\bar{b}$ channels, which are PDF suppressed, though not changing the size of the NLO EW corrections, gives a 12% increase to the LL cross section. The corresponding contribution for mixed states is at the 3% level, while it is completely negligible for the TT state. This effect comes from the presence of a t-channel top quark that leads to a different helicity structure contributing to the LO amplitude, favouring a longitudinal mode for the W bosons. Including the $b\bar{b}$ contributions does not change the relative size of off-shell and interference effects.

For completeness, we have evaluated the full off-shell process including also $\gamma b\,(\gamma\bar{b})$ channels, which are characterised by (anti)top quarks in the s channel. These photon-induced corrections account for almost 5% of the full off-shell NLO EW cross section in the five-flavour scheme. Dominated by the presence of (anti)top quarks, these contributions constitute an irreducible background to EW production of W^+W^-. A similar reasoning holds for gb, $g\bar{b}$ and gg channels that arise at NLO and NNLO in QCD, respectively. The combination of EW and QCD corrections, although indispensable for a realistic and precise SM modelling, falls outside the scope of this letter and is left for future work.

In order to experimentally separate polarisation states for intermediate EW bosons, it is necessary to model precisely the polarised signals in terms of differential observables, identifying those that provide the highest discrimination power. We present differential results for three kinematic variables: the first one relies on the use of neutrino momenta from Monte Carlo truth, while the second and the third ones are LHC observables. While we incorporate the $b\bar{b}$ channels in all distributions, we do not include the γb, $\gamma\bar{b}$ channels therein, but instead show their contribution to the full off-shell results separately.

In Fig. 2 we present distributions in the cosine of the polar decay angle of the positron in the W^+ rest frame, which relies on the (unphysical) reconstruction of individual W bosons. As proven by the normalised shapes, this quantity gives the highest sensitivity to the polarisation state of the W^+ boson, while it is rather agnostic of the polarisation state of the W^- boson. The NLO EW corrections for the various states reflect those found at the integrated level (see Table 1), with some deviation from the flat behaviour just in the anticollinear regime, which is the least populated one. In this regime, the TT and TL signals would

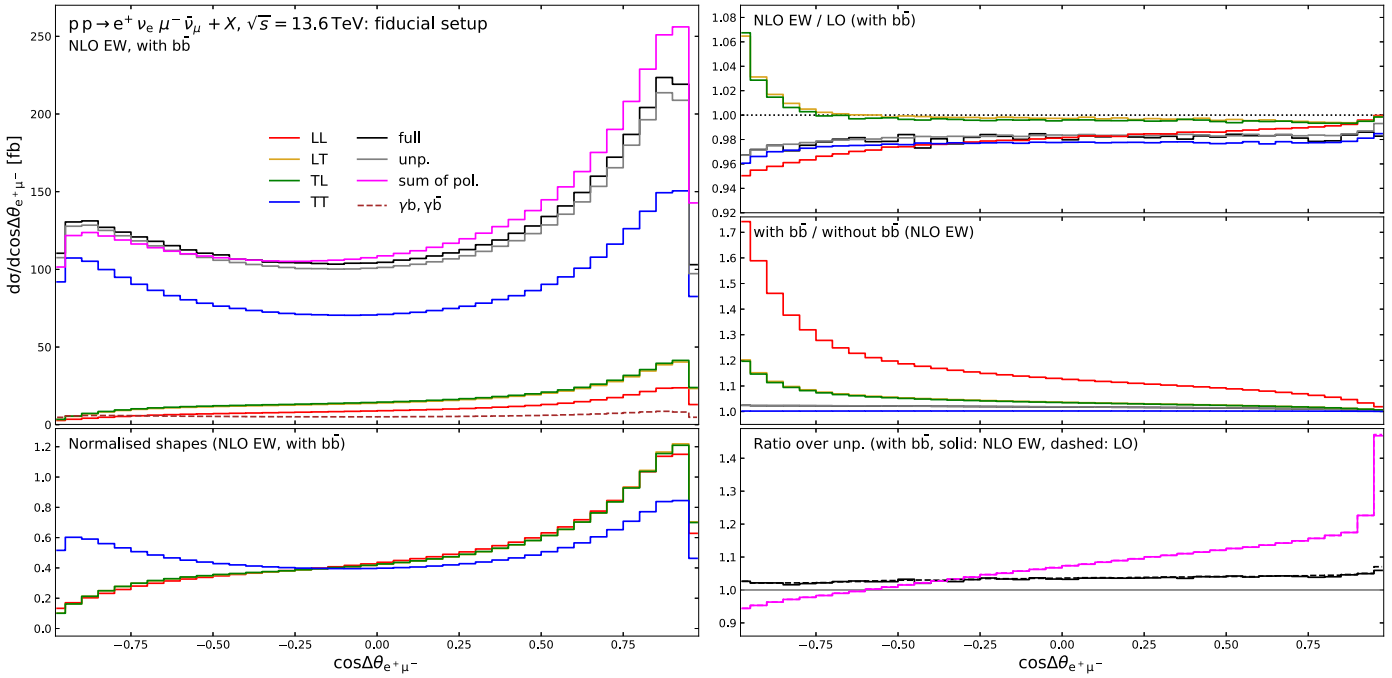

Fig. 3. Distributions in the cosine of the angular separation between the positron and the muon for W^+W^- production and decay at the LHC with NLO EW accuracy. Same structure as Fig. 2.

have a maximum in the absence of cuts (driven by the favoured left-handed polarisation), while the transverse-momentum selection on the positron distorts dramatically the shape emptying this region. The impact of $b\bar{b}$ channels, negligible for the TT state, increases towards the collinear regime for the longitudinal W^- states (LL, TL). The off-shell effects are flat in most of the angular range, while they increase up to 15% in the anticollinear regime. The interferences, already found to be large for polarisations defined in the laboratory frame [6,10], are enhanced in the central region of the spectrum, *i.e.* $\theta^{*,\mathrm{CM}}_{e^+} \approx \pi/2$, where they amount to 13%. These large effects are known to come from the application of p_T cuts on the kinematics of the positron, which prevents the interference between longitudinal and transverse modes of the W^+ boson from integrating to zero [50].

In Fig. 3 we present the distributions in an angular observable that can be fully accessed at the LHC, namely the angular separation between the two charged leptons, computed in the laboratory frame. The shapes for the LL and mixed states clearly suggest that the two leptons are preferably produced collinear to each other, with a sharp drop in the rightmost bin that is motivated by the fiducial invariant-mass selection ($M_{e^+\mu^-} > 20\,\mathrm{GeV}$), while the anticollinear regime is disfavoured. A different behaviour is found for the TT distribution, whose shape presents two local maxima close to both the collinear (absolute maximum) and to the anticollinear regimes. The NLO EW corrections for the LL state increase from −5% to −0.1% towards the collinear regime, those for the TT state are comparably flat. The mixed states are both characterised by positive corrections (up to 6.5%) in the anticollinear region, but almost negligible ones in the rest of the angular range. The relative impact of $b\bar{b}$ contributions to the LL state is maximal in the anticollinear region (more than 75% for $\Delta\theta_{e^+\mu^-} \approx \pi$) and decreases monotonically towards the collinear region (most populated one). A similar trend, though overall less sizeable, is found for the LT and TL states. While the off-shell effects are flat, the interference pattern is strikingly interesting, with a linear decrease from +5% to −17% towards the collinear region, and a deviation from this constant slope just in the very last bins (up to 45% effect). A similar interference pattern has been observed also in the distributions in the azimuthal-angle separation between the two charged leptons.

In Fig. 4 we analyse the distributions in the invariant mass of the positron–muon system. Similarly to the discussion of the previous observable, the normalised TT shape markedly deviates from the one found for other doubly polarised states, with a different maximum position ($M_{e^+\mu^-} \approx 50\,\mathrm{GeV}$ for TT, $\approx 65\,\mathrm{GeV}$ for other states). The TT state dominates the unpolarised cross section with a decrease by 1.5 orders of magnitude between its maximum position and 400 GeV. The suppression of the other states towards large invariant-mass values is more marked, with a decrease by more than two orders of magnitude in the same mass range. The LL distribution exceeds the mixed ones already at a smaller invariant mass ($\approx 270\,\mathrm{GeV}$) than for polarised states defined in the laboratory frame [6]. The NLO EW corrections are increasingly negative for the LL and TT states towards large invariant mass, showing the expected enhancement from large logarithms of EW origin. On the contrary, the positively increasing EW corrections at moderate-to-large mass found for the LT and TL distributions mostly come from a LO suppression of these states, which results from unitarity cancellations and is proportional to the energy of the longitudinal W boson [51]. The impact of the $b\bar{b}$ channel becomes very large at moderate values of $M_{e^+\mu^-}$ (+50% at 200 GeV for LL). The off-shell effects mildly vary between 3% and 8% in the considered range. The interferences vanish for larger mass, while they rapidly increase approaching the minimum mass value allowed by the selections (40% at the 20-GeV cut).

5. Conclusions

We have presented the first calculation of NLO EW corrections to doubly polarised W^+W^- production at the LHC in the decay channel with two opposite-sign, different-flavour leptons. Using the double-pole approximation to extract the WW-resonant contributions out of the full off-shell cross section and selecting polarisation states for intermediate bosons in the tree-level and one-loop amplitudes, we have calculated integrated and differential cross sections for various polarised states and drawn phenomenological consequences relevant for the LHC Run-3 analysis programme. We have carried out the calculation in the five-flavour scheme, finding non-negligible contributions from the $b\bar{b}$-induced partonic channel, especially for the purely longitudinal state. The NLO EW corrections at integrated level for the doubly polarised

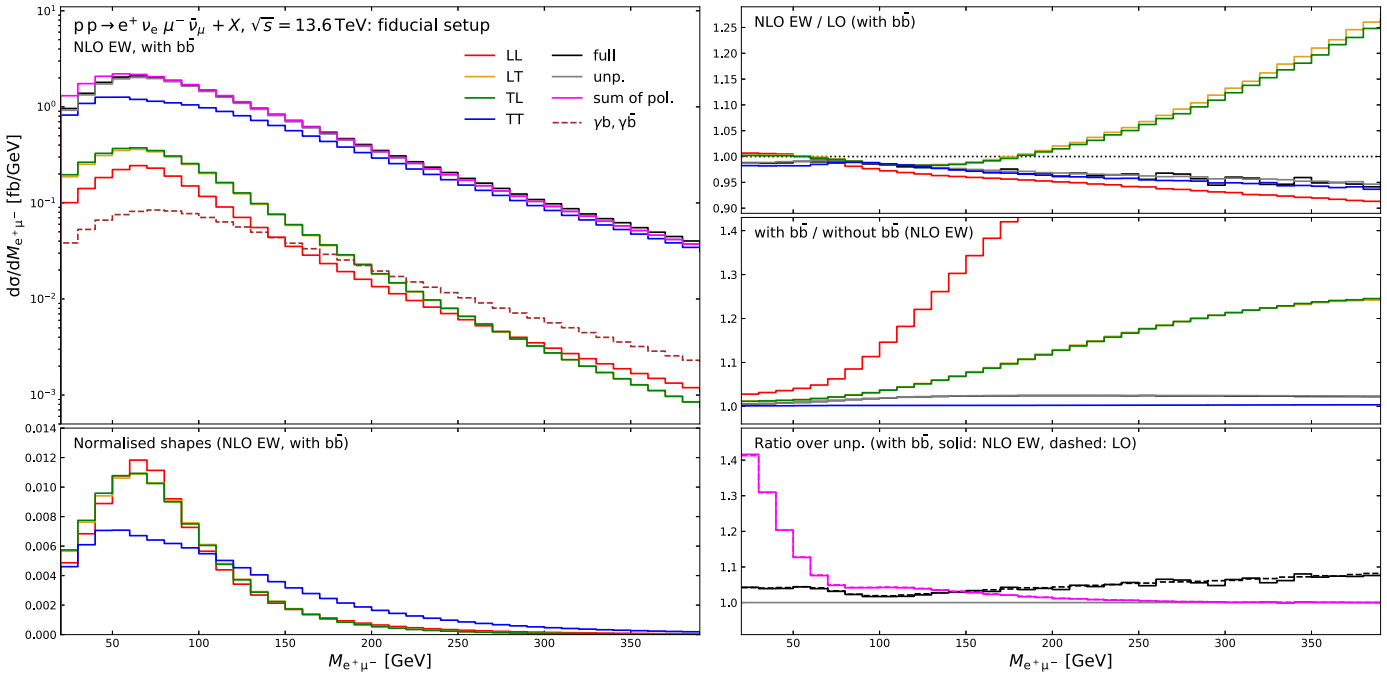

Fig. 4. Distributions in the invariant mass of the positron–muon pair for W^+W^- production and decay at the LHC with NLO EW accuracy. Same structure as Fig. 2.

states range from −0.3% for mixed states to −1.7% for the purely longitudinal one to −2.4% for the purely transverse one. Much larger EW corrections characterise the tails of invariant-mass distributions, with typical enhancement from EW logarithms in the same-polarisation states and positively increasing corrections for the mixed states owing to a LO suppression. Some observables, both angular and energy-dependent, have been found to have a marked discrimination power among polarisations, and therefore to be suitable for polarised-template fits of LHC data, even in a challenging process like W^+W^-.

Note added

One day after we made this letter public on arXiv, another calculation of NLO EW corrections to polarised W^+W^- production appeared [52] by T. N. Dao and D. N. Le. This calculation differs from ours by the LHC centre-of-mass energy and the applied kinematic selections.

Declaration of competing interest

The authors declare the following financial interests/personal relationships which may be considered as potential competing interests: Ansgar Denner reports financial support was provided by German Federal Ministry for Education and Research (BMBF). Ansgar Denner reports financial support was provided by German Research Foundation (DFG). Christoph Haitz reports financial support was provided by German Federal Ministry for Education and Research (BMBF). Christoph Haitz reports financial support was provided by German Research Foundation (DFG). If there are other authors, they declare that they have no known competing financial interests or personal relationships that could have appeared to influence the work reported in this paper.

Data availability

Data will be made available on request.

Acknowledgements

The authors are grateful to Jean-Nicolas Lang and Sandro Uccirati for maintaining RECOLA. GP thanks Giulia Zanderighi and Rene Poncelet for useful discussions. The authors acknowledge support from the COMETA COST Action CA22130. This work is supported by the German Federal Ministry for Education and Research (BMBF) under contract no. 05H21WWCAA and by the German Research Foundation (DFG) under reference number DFG 623/8-1.

References

[1] M. Aaboud, et al., Measurement of $W^{\pm}Z$ production cross sections and gauge boson polarisation in pp collisions at $\sqrt{s} = 13$ TeV with the ATLAS detector, Eur. Phys. J. C 79 (6) (2019) 535, https://doi.org/10.1140/epjc/s10052-019-7027-6, arXiv:1902.05759.

[2] A.M. Sirunyan, et al., Measurements of production cross sections of polarized same-sign W boson pairs in association with two jets in proton-proton collisions at $\sqrt{s} =$ 13 TeV, Phys. Lett. B 812 (2021) 136018, https://doi.org/10.1016/j.physletb.2020.136018, arXiv:2009.09429.

[3] A. Tumasyan, et al., Measurement of the inclusive and differential WZ production cross sections, polarization angles, and triple gauge couplings in pp collisions at $\sqrt{s}$ =13 TeV, J. High Energy Phys. 07 (2022) 032, https://doi.org/10.1007/JHEP07(2022)032, arXiv:2110.11231.

[4] G. Aad, et al., Observation of gauge boson joint-polarisation states in $W^{\pm}Z$ production from pp collisions at $\sqrt{s} = 13$ TeV with the ATLAS detector, Phys. Lett. B 843 (2023) 137895, https://doi.org/10.1016/j.physletb.2023.137895, arXiv:2211.09435.

[5] G. Aad, et al., Evidence of pair production of longitudinally polarised vector bosons and study of CP properties in $ZZ \to 4\ell$ events with the ATLAS detector at $\sqrt{s} = 13$ TeV, J. High Energy Phys. 12 (2023) 107, https://doi.org/10.1007/JHEP12(2023)107, arXiv:2310.04350.

[6] A. Denner, G. Pelliccioli, Polarized electroweak bosons in W^+W^- production at the LHC including NLO QCD effects, J. High Energy Phys. 09 (2020) 164, https://doi.org/10.1007/JHEP09(2020)164, arXiv:2006.14867.

[7] A. Denner, G. Pelliccioli, NLO QCD predictions for doubly-polarized WZ production at the LHC, Phys. Lett. B 814 (2021) 136107, https://doi.org/10.1016/j.physletb.2021.136107, arXiv:2010.07149.

[8] A. Denner, C. Haitz, G. Pelliccioli, NLO QCD corrections to polarized diboson production in semileptonic final states, Phys. Rev. D 107 (5) (2023) 053004, https://doi.org/10.1103/PhysRevD.107.053004, arXiv:2211.09040.

[9] M. Hoppe, M. Schönherr, F. Siegert, Polarised cross sections for vector boson production with SHERPA, arXiv:2310.14803, 10 2023.

[10] R. Poncelet, A. Popescu, NNLO QCD study of polarised W^+W^- production at the LHC, J. High Energy Phys. 07 (2021) 023, https://doi.org/10.1007/JHEP07(2021)023, arXiv:2102.13583.

[11] A. Denner, G. Pelliccioli, NLO EW and QCD corrections to polarized ZZ production in the four-charged-lepton channel at the LHC, J. High Energy Phys. 10 (2021) 097, https://doi.org/10.1007/JHEP10(2021)097, arXiv:2107.06579.

[12] D.N. Le, J. Baglio, T.N. Dao, Doubly-polarized WZ hadronic production at NLO QCD+EW: calculation method and further results, Eur. Phys. J. C 82 (12) (2022) 1103, https://doi.org/10.1140/epjc/s10052-022-11032-2, arXiv:2208.09232.

[13] D.N. Le, J. Baglio, Doubly-polarized WZ hadronic cross sections at NLO QCD + EW accuracy, Eur. Phys. J. C 82 (10) (2022) 917, https://doi.org/10.1140/epjc/s10052-022-10887-9, arXiv:2203.01470.

[14] T.N. Dao, D.N. Le, Enhancing the doubly-longitudinal polarization in WZ production at the LHC, Commun. Phys. 33 (3) (2023) 223, https://doi.org/10.15625/0868-3166/18077, arXiv:2302.03324.

[15] F. Caola, K. Melnikov, R. Röntsch, L. Tancredi, QCD corrections to W^+W^- production through gluon fusion, Phys. Lett. B 754 (2016) 275–280, https://doi.org/10.1016/j.physletb.2016.01.046, arXiv:1511.08617.

[16] M. Grazzini, S. Kallweit, S. Pozzorini, D. Rathlev, M. Wiesemann, W^+W^- production at the LHC: fiducial cross sections and distributions in NNLO QCD, J. High Energy Phys. 08 (2016) 140, https://doi.org/10.1007/JHEP08(2016)140, arXiv:1605.02716.

[17] M. Grazzini, S. Kallweit, J.M. Lindert, S. Pozzorini, M. Wiesemann, NNLO QCD + NLO EW with Matrix+OpenLoops: precise predictions for vector-boson pair production, J. High Energy Phys. 02 (2020) 087, https://doi.org/10.1007/JHEP02(2020)087, arXiv:1912.00068.

[18] M. Billoni, S. Dittmaier, B. Jäger, C. Speckner, Next-to-leading order electroweak corrections to pp → W^+W^- → 4 leptons at the LHC in double-pole approximation, J. High Energy Phys. 12 (2013) 043, https://doi.org/10.1007/JHEP12(2013)043, arXiv:1310.1564.

[19] B. Biedermann, M. Billoni, A. Denner, S. Dittmaier, L. Hofer, B. Jäger, L. Salfelder, Next-to-leading-order electroweak corrections to $pp \to W^+W^- \to 4$ leptons at the LHC, J. High Energy Phys. 06 (2016) 065, https://doi.org/10.1007/JHEP06(2016)065, arXiv:1605.03419.

[20] M. Chiesa, C. Oleari, E. Re, NLO QCD+NLO EW corrections to diboson production matched to parton shower, Eur. Phys. J. C 80 (9) (2020) 849, https://doi.org/10.1140/epjc/s10052-020-8419-3, arXiv:2005.12146.

[21] S. Bräuer, A. Denner, M. Pellen, M. Schönherr, S. Schumann, Fixed-order and merged parton-shower predictions for WW and WWj production at the LHC including NLO QCD and EW corrections, J. High Energy Phys. 10 (2020) 159, https://doi.org/10.1007/JHEP10(2020)159, arXiv:2005.12128.

[22] D. Lombardi, M. Wiesemann, G. Zanderighi, W^+W^- production at NNLO+PS with MINNLO$_{PS}$, J. High Energy Phys. 11 (2021) 230, https://doi.org/10.1007/JHEP11(2021)230, arXiv:2103.12077.

[23] G. Pelliccioli, G. Zanderighi, Polarised-boson pairs at the LHC with NLOPS accuracy, Eur. Phys. J. C 84 (1) (2024) 16, https://doi.org/10.1140/epjc/s10052-023-12347-4, arXiv:2311.05220.

[24] R.G. Stuart, Gauge invariance, analyticity and physical observables at the Z^0 resonance, Phys. Lett. B 262 (1991) 113–119, https://doi.org/10.1016/0370-2693(91)90653-8.

[25] A. Aeppli, F. Cuypers, G.J. van Oldenborgh, $\mathcal{O}(\Gamma)$ corrections to W pair production in e^+e^- and $\gamma\gamma$ collisions, Phys. Lett. B 314 (1993) 413–420, https://doi.org/10.1016/0370-2693(93)91259-P, arXiv:hep-ph/9303236.

[26] A. Aeppli, G.J. van Oldenborgh, D. Wyler, Unstable particles in one loop calculations, Nucl. Phys. B 428 (1994) 126–146, https://doi.org/10.1016/0550-3213(94)90195-3, arXiv:hep-ph/9312212.

[27] A. Denner, S. Dittmaier, M. Roth, D. Wackeroth, Electroweak radiative corrections to $e^+e^- \to WW \to 4$ fermions in double pole approximation: the RACOONWW approach, Nucl. Phys. B 587 (2000) 67–117, https://doi.org/10.1016/S0550-3213(00)00511-3, arXiv:hep-ph/0006307.

[28] S. Catani, M.H. Seymour, A general algorithm for calculating jet cross-sections in NLO QCD, Nucl. Phys. B 485 (1997) 291–419, https://doi.org/10.1016/S0550-3213(96)00589-5, Nucl. Phys. B 510 (1998) 503 (Erratum), arXiv:hep-ph/9605323.

[29] S. Dittmaier, A general approach to photon radiation off fermions, Nucl. Phys. B 565 (2000) 69–122, https://doi.org/10.1016/S0550-3213(99)00563-5, arXiv:hep-ph/9904440.

[30] S. Catani, S. Dittmaier, M.H. Seymour, Z. Trocsanyi, The dipole formalism for next-to-leading order QCD calculations with massive partons, Nucl. Phys. B 627 (2002) 189–265, https://doi.org/10.1016/S0550-3213(02)00098-6, arXiv:hep-ph/0201036.

[31] S. Dittmaier, A. Kabelschacht, T. Kasprzik, Polarized QED splittings of massive fermions and dipole subtraction for non-collinear-safe observables, Nucl. Phys. B 800 (2008) 146–189, https://doi.org/10.1016/j.nuclphysb.2008.03.010, arXiv:0802.1405.

[32] M. Schönherr, An automated subtraction of NLO EW infrared divergences, Eur. Phys. J. C 78 (2018) 119, https://doi.org/10.1140/epjc/s10052-018-5600-z, arXiv:1712.07975.

[33] S. Dittmaier, C. Schwan, Non-factorizable photonic corrections to resonant production and decay of many unstable particles, Eur. Phys. J. C 76 (2016) 144, https://doi.org/10.1140/epjc/s10052-016-3968-1, arXiv:1511.01698.

[34] A. Denner, S. Dittmaier, Electroweak radiative corrections for collider physics, Phys. Rep. 864 (2020) 1–163, https://doi.org/10.1016/j.physrep.2020.04.001, arXiv:1912.06823.

[35] A. Denner, S. Dittmaier, M. Roth, Nonfactorizable photonic corrections to $e^+e^- \to WW \to 4$ fermions, Nucl. Phys. B 519 (1998) 39–84, https://doi.org/10.1016/S0550-3213(98)00046-7, arXiv:hep-ph/9710521.

[36] S. Actis, A. Denner, L. Hofer, A. Scharf, S. Uccirati, Recursive generation of one-loop amplitudes in the standard model, J. High Energy Phys. 04 (2013) 037, https://doi.org/10.1007/JHEP04(2013)037, arXiv:1211.6316.

[37] S. Actis, A. Denner, L. Hofer, J.-N. Lang, A. Scharf, S. Uccirati, RECOLA: REcursive computation of one-loop amplitudes, Comput. Phys. Commun. 214 (2017) 140–173, https://doi.org/10.1016/j.cpc.2017.01.004, arXiv:1605.01090.

[38] A. Denner, S. Dittmaier, L. Hofer, COLLIER: a fortran-based complex one-loop LIbrary in extended regularizations, Comput. Phys. Commun. 212 (2017) 220–238, https://doi.org/10.1016/j.cpc.2016.10.013, arXiv:1604.06792.

[39] V. Hirschi, R. Frederix, S. Frixione, M.V. Garzelli, F. Maltoni, R. Pittau, Automation of one-loop QCD corrections, J. High Energy Phys. 05 (2011) 044, https://doi.org/10.1007/JHEP05(2011)044, arXiv:1103.0621.

[40] R.L. Workman, et al., Review of particle physics, PTEP 2022 (2022) 083C01, https://doi.org/10.1093/ptep/ptac097.

[41] D.Yu. Bardin, A. Leike, T. Riemann, M. Sachwitz, Energy-dependent width effects in e^+e^--annihilation near the Z-boson pole, Phys. Lett. B 206 (1988) 539–542, https://doi.org/10.1016/0370-2693(88)91627-9.

[42] S. Dittmaier, M. Krämer, Electroweak radiative corrections to W-boson production at hadron colliders, Phys. Rev. D 65 (2002) 073007, https://doi.org/10.1103/PhysRevD.65.073007, arXiv:hep-ph/0109062.

[43] A. Denner, S. Dittmaier, M. Roth, L.H. Wieders, Electroweak corrections to charged-current $e^+e^- \to 4$ fermion processes: technical details and further results, Nucl. Phys. B 724 (2005) 247–294, https://doi.org/10.1016/j.nuclphysb.2011.09.001, Nucl. Phys. B 854 (2012) 504, https://doi.org/10.1016/j.nuclphysb.2005.06.033 (Erratum), arXiv:hep-ph/0505042.

[44] A. Denner, S. Dittmaier, The complex-mass scheme for perturbative calculations with unstable particles, Nucl. Phys. B, Proc. Suppl. 160 (2006) 22–26, https://doi.org/10.1016/j.nuclphysbps.2006.09.025, arXiv:hep-ph/0605312.

[45] R.D. Ball, et al., Parton distributions from high-precision collider data, Eur. Phys. J. C 77 (10) (2017) 663, https://doi.org/10.1140/epjc/s10052-017-5199-5, arXiv:1706.00428.

[46] V. Bertone, S. Carrazza, N.P. Hartland, J. Rojo, Illuminating the photon content of the proton within a global PDF analysis, SciPost Phys. 5 (2018) 008, https://doi.org/10.21468/SciPostPhys.5.1.008, arXiv:1712.07053.

[47] A. Buckley, J. Ferrando, S. Lloyd, K. Nordström, B. Page, M. Rüfenacht, M. Schönherr, G. Watt, LHAPDF6: parton density access in the LHC precision era, Eur. Phys. J. C 75 (2015) 132, https://doi.org/10.1140/epjc/s10052-015-3318-8, arXiv:1412.7420.

[48] A.M. Sirunyan, et al., W^+W^- boson pair production in proton-proton collisions at $\sqrt{s} = 13$ TeV, Phys. Rev. D 102 (9) (2020) 092001, https://doi.org/10.1103/PhysRevD.102.092001, arXiv:2009.00119.

[49] M. Cacciari, G.P. Salam, G. Soyez, The anti-k_t jet clustering algorithm, J. High Energy Phys. 04 (2008) 063, https://doi.org/10.1088/1126-6708/2008/04/063, arXiv:0802.1189.

[50] A. Ballestrero, E. Maina, G. Pelliccioli, W boson polarization in vector boson scattering at the LHC, J. High Energy Phys. 03 (2018) 170, https://doi.org/10.1007/JHEP03(2018)170, arXiv:1710.09339.

[51] S.S.D. Willenbrock, Pair production of W and Z bosons and the Goldstone boson equivalence theorem, Ann. Phys. 186 (1988) 15, https://doi.org/10.1016/S0003-4916(88)80016-2.

[52] T.N. Dao, D.N. Le, NLO electroweak corrections to doubly-polarized W^+W^- production at the LHC, arXiv:2311.17027, 11 2023.